SMELTING OF LOW-GRADE SAPROLITIC NICKEL ORE IN DC-ARC FURNACE

F. Nurjaman [a, *], H.Z. Hakim [b], B. Septiansyah [b], L.O. Arham [b], A.S. Handoko [a], F. Bahfie [a], I. Suherman [a], H. Haryadi [a], T. Suseno [a], Y. Sari [a], B. Suharno [c]

[a] National Research and Innovation Agency, Research Center for Mining Technology, South Lampung, Indonesia
[b] Insitut Teknologi Sumatera, Department of Mining Engineering, , South Lampung, Indonesia
[c] Universitas Indonesia, Department of Metallurgy and Material, Depok, Indonesia

Abstract

Most nickel laterite smelting to produce ferronickel is carried out using an AC-arc furnace. Although the DC-arc furnace is advantageous in the smelting of fine ore, it is rarely used for nickel laterite. In this work, the effects of slag basicity and stoichiometry of reductant addition during smelting of low-grade saprolitic nickel ore on nickel content and nickel recovery, yield, and phases of the slag were studied in detail. The smelting process was conducted in a laboratory DC-arc furnace with a a single electrode of 30 cm diameter. A 5 kg of low-grade saprolitic nickel ore (1.92 Ni-12.97 Fe), some coke as reductant, and some limestone as flux were smelted in a DC-arc furnace for about one hour. The pouring temperature of hot metal and slag was 1400-1500 °C. The basicity of the quaternary slag of 0.8 and the stoichiometric carbon of 0.8 of the reductant resulted in an optimum smelting process of nickel ore in a DC-arc furnace, producing ferronickel with a Ni content of 14.59% with 92.26% recovery.

Keywords: Nickel laterite; Smelting; DC-arc furnace; Ferronickel

1. Introduction

Nickel is one of the most strategic metals in the world. Almost 65% of metallic nickel is used for stainless steel production in the form of ferronickel, replacing the expensive electrolytic nickel [1]. Nickel sulfide has been mainly processed for ferronickel production for many years due to its high nickel content, especially after the physical beneficiation process. Nevertheless, the depletion of nickel sulfide reserves has made some industries switch their attention to nickel laterite. However, it is more challenging in its processing because it has low nickel content and also contains high water and impurities, which results in high consumption energy of the smelting process [2]. According to Tsang and Zhang, the energy cost is approximately 50% of the total nickel production cost using RKEF [3], which is equivalent to 460 GJ per metric ton Ni in product [4].
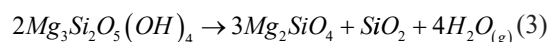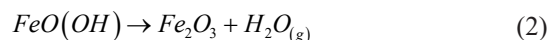
Ferronickel can be obtained from saprolitic nickel laterite by the carbothermic reduction process [5]. Carbonaceous material, such as coke or coal, is mostly used to reduce the metallic oxide into the metallic phase. The rotary kiln electric furnace (RKEF) is a well-proven technology for smelting nickel laterite into ferronickel [6]. The process consisted of ore drying in a rotary dryer, (reaction (1)); dehydroxylation (reaction (2-3)); and indirect pre-reduction of some metallic oxide in a rotary kiln at 700 °C, (reaction (4-8)) [7], then continued with smelting process in a submerged AC-arc furnace about 1500-1600 °C which involves the indirect and direct reduction process, (reaction (9-13)) [8].
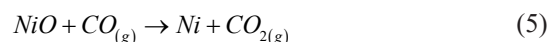
Drying in the rotary dryer:

$$H_2O_{(l)} \rightarrow H_2O_{(g)} \tag{1}$$

Dehydroxylation process in a rotary kiln:

$$FeO(OH) \rightarrow Fe_2O_3 + H_2O_{(g)} \tag{2}$$
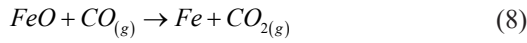
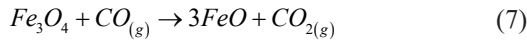$$2Mg_3Si_2O_5(OH)_4 \rightarrow 3Mg_2SiO_4 + SiO_2 + 4H_2O_{(g)} \tag{3}$$

Indirect reduction in a rotary kiln:

$$C + CO_{2(g)} \rightarrow 2CO_{(g)} \tag{4}$$

$$NiO + CO_{(g)} \rightarrow Ni + CO_{2(g)} \tag{5}$$

$$3Fe_2O_3 + CO_{(g)} \rightarrow 2Fe_3O_4 + CO_{2(g)} \qquad (6)$$

$$Fe_3O_4 + CO_{(g)} \rightarrow 3FeO + CO_{2(g)} \qquad (7)$$

$$FeO + CO_{(g)} \rightarrow Fe + CO_{2(g)} \qquad (8)$$
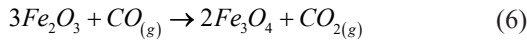
Direct reduction in the electric furnace:

$$3Fe_2O_3 + C \rightarrow 2Fe_3O_4 + CO_{(g)} \qquad (9)$$

$$Fe_3O_4 + C \rightarrow 3FeO + CO_{(g)} \qquad (10)$$

$$FeO + C \rightarrow Fe + CO_{(g)} \qquad (11)$$

$$NiO + C \rightarrow Ni + CO_{(g)} \qquad (12)$$

$$Fe + Ni \rightarrow FeNi \qquad (13)$$
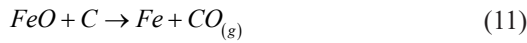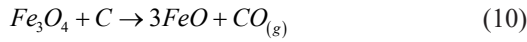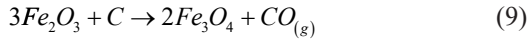
Some efforts for reducing the consumption energy of nickel laterite smelting in RKEF were carried out by selecting or treating the input materials, such as the Fe/Ni, Ni/Co, SiO$_2$/MgO ratio of nickel ore should be <2.0, >30, <1.9, respectively. The iron content must not exceed 20% to avoid slag foaming, which could promote operational instability resulting in decreased power and production levels [9-10]. Controlling the slag basicity in nickel laterite smelting using an AC-arc furnace in the RKEF also can reduce energy consumption by promoting the formation of low melting point phases, such as diopside and olivine eutectic, by adjusting the quaternary of slag basicity ((CaO+MgO)/(SiO$_2$+Al$_2$O$_3$)) about 0.58 to 0.61. as a result, the energy consumption in the smelting of saprolitic nickel ore could be reduced from 13.5 to 11.16 GJ/ton [11]. Andika et al. (2019) also reported that the optimum quaternary basicity of 1.0 was obtained in the smelting of uncalcined limonitic nickel ore with 1.24 Ni-43.1 Fe in Submerged AC-arc furnace by using coke as a reductant producing ferronickel contain 4% Ni with 89% recovery [12].

The DC-arc furnace is less used for nickel laterite smelting due to its furnace characteristic, which requires higher energy consumption caused by the radiation heat loss through the furnace and the walls during the open bath smelting process [13]. Nevertheless, the reduction in energy consumption can be achieved by making some improvements in the furnace design, such as the utilization of waste heat or combustible flue gas from the furnace for firing in a rotary dryer or rotary kiln in the pre-reduction of nickel ore prior to the smelting process [14-15]. In nickel smelting, the drying and calcination processes usually generate so much nickel ore dust, which is challenging to smelt in a submerged AC-arc furnace. The DC-arc furnace has several advantages over the submerged AC-electric arc furnace [16-17]. It can melt fine particles of less than 0.1 mm due to the open

bath process, which could reduce the energy or cost required to agglomerate fine nickel laterite before charging into the furnace [18]. DC-arc furnace has lower electrode consumption and smaller diameter with the same current due to the "skin effect" experienced in an AC-arc furnace [19]. Therefore, replacing the three-phase AC (alternating current)-arc furnace with single phase DC (direct current)-arc furnace can be profitable. In this work, the effect of reductant dosage and slag basicity in smelting saprolitic nickel laterite has been investigated clearly.

2. Materials, Equipment, and Method
2.1. Materials

Nickel laterite was obtained from Southeast Sulawesi, Indonesia. The chemical composition of this nickel ore is listed in Table 1 It has a high content of magnesium oxide and silicon dioxide, but a low content of iron and nickel. The XRD analysis in Figure 1 and the Rietveld analysis in Table 2 show that the mineral compound is dominated by magnesium silicate oxide and hydroxide, which refers to saprolitic nickel ore. In saprolite, iron and nickel are associated with magnesium silicate structure, i.e., lizardite, forsterite, and enstatite, replacing the magnesium atom, causing it more challenging to reduce into metallic iron compared to goethite ((Fe, Ni)OOH), which is mostly found in limonitic nickel ore [20]. Generally, saprolite contains 2-5% nickel [21]. Less than 2.4% Ni is classified as low-grade saprolitic nickel ore [22]. In this work, saprolite with 1.97% Ni and 12.97% Fe was used.

Coke and limestone were added in this smelting process as reductant and flux, respectively. The analysis of the coke and the chemical composition of limestone is listed in Tables 3 and 4. In this work, the carbon required for reducing the metal oxide was calculated based on stoichiometric of mole ratio in reaction (9-12). The amount of coke was added by divided the total of carbon required by the fix carbon content in coke. The quaternary basicity (R$_4$) of the slag is used in this experiment, as expressed in equation (14). Limestone was added to modify the basicity.

$$R_4 = \frac{(CaO + MgO)}{(SiO_2 + Al_2O_3)} \qquad (14)$$

2.2. DC-Arc Furnace

In this work, the DC-arc furnace (Figure 2(b)) has a single graphite electrode as the cathode with a

Table 1. *Chemical composition of nickel laterite*

Elements/Compounds (wt %)							Basicity (R$_4$)
Fe	Ni	Cr	MgO	SiO$_2$	CaO	Al$_2$O$_3$	
12.97	1.92	0.42	11.26	43.24	0.84	1.33	0.28
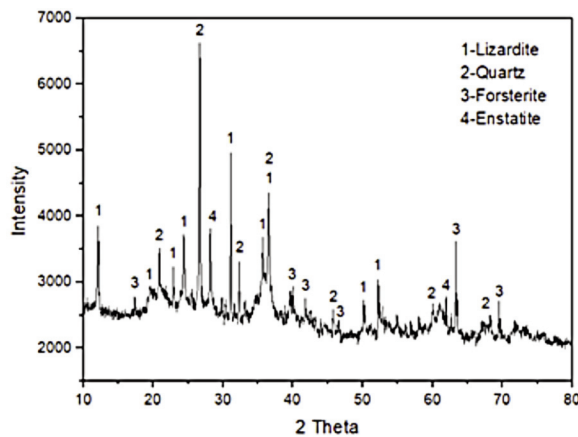
Figure 1. XRD analysis of nickel laterite

Table 2. *Rietveld analysis of nickel laterite*

Compounds	wt %
Quartz-SiO_2	20.3
Lizardite-$Mg_3 Si_2O_5(OH)_4$	25.3
Forsterite (Ni-Fe)-(Fe,Ni)MgSi O_4	22.2
Enstatite-$MgSiO_3$	32.1

Table 3. *Proximate, sulfur, and calorie analysis of coke*

Proximate analysis (wt %)				Sulfur (wt %)	Calorie Value (Cal/gr)
Moisture	Volatile Matter	Ash Content	Fix Carbon		
0.72	2.63	22.47	74.17	0.97	6332

Table 4. *Chemical analysis of limestone*

Compounds	$CaCO_3$	Fe_2O_3	MnO	MgO	SiO_2	Al_2O_3	P_2O_5
wt %	73.7	5.1	0.01	1	8.3	6.8	0.4

diameter of 30 mm, while the graphite anode is located at the bottom of the furnace. The chamber size is Ø200 mm x 400 mm, which corresponds to 10 kg of raw materials (nickel ore, coke, and limestone). The chamber was insulated with alumina castable, which made contact with liquid metal slag, and with firebricks as a second layer. It is an open furnace, there is no rooftop above the chamber. The electric current of 20-30 ampere flows to the 40-volt transformer, resulting in current output of about 400-

600 ampere. A submerged thermocouple (with a maximum measurement up to 1700 °C) was used to measure the hot metal before pouring.

Table 5. *Composition of raw materials*

No.	Composition (kg)			Stoichiometry of reductant	Slag basicity
	Nickel ore	Limestone	Coke		
1	5	0.7	0.35	1	0.6
2	5	1.2	0.35	1	0.8
3	5	1.6	0.35	1	1
4	5	2	0.35	1	1.2
5	5	1.2	0.2	0.6	0.8
6	5	1.2	0.25	0.8	0.8
7	5	1.2	0.35	1	0.8
8	5	1.2	0.4	1.2	0.8

2.3. Experiment

The saprolitic nickel ore, which varied in size from 30 mm to less than 1 mm, was dried at 120 °C for 4 hours to release the moisture. No-calcination process was conducted before the smelting of nickel ore. As listed in Table 5 and shown in Figure 2(a), nickel ore, coke, and limestone were smelted in a DC-arc furnace at 1450-1500 °C. The smelting process took 60 minutes. Furthermore, the liquid ferronickel and slag were poured from a single tap hole, as shown in Figure 2(c). The chemical composition of ferronickel and slag was analyzed using spark optical emission spectrometry (OES) and X-ray fluorescence (XRF), respectively, to identify the grade and recovery of ferronickel. The X-ray diffraction (XRD) analysis was used to observe the phases of slag, and a secondary electron microscope (SEM) equipped with energy dispersive X-ray (EDX) was used for to identify the microstructure of ferronickel.

The recovery of iron and nickel was calculated by using Equation (15). In this work, the effect of reductant dosage and slag basicity level on the smelting of nickel ore with a DC-arc furnace was carried out by adjusting coke and limestone addition
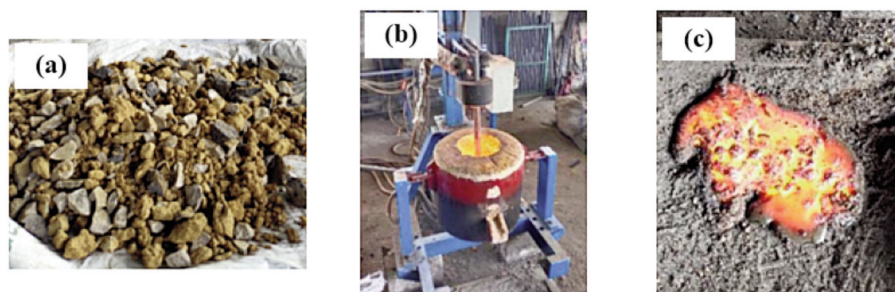

Figure 2. (a) raw materials (nickel ore, coke, and limestone); (b) DC-arc furnace; (c) hot metal and slag

from 0.6-1.2 stoichiometry and 0.6 to 1.2 basicity, respectively, as listed in Table 5. The stoichiometry reductant means carbon needs for reaction (1-5) in the equilibrium state.

$$\text{Recovery}\,(R)_{Fe,Ni} = \frac{\%wt.\,(Fe,\text{Ni})\,in\,FeNi \cdot wt.\,of\,FeNi(gr)}{\%wt.FeNi\,in\,nickel\,ore \cdot 5000\,(gr)}\,(15)$$

3. Result and Discussion

Reductant and basicity play an important role in smelting, contributing to the successful nickel extraction from nickel laterite. A sufficient reductant amount should be added to reduce metallic oxide, and the proper slag basicity should be determined to obtain a low melting point phase resulting in low energy consumption. Therefore, the effect of slag basicity and reductant in smelting nickel ore by using a DC-arc furnace was comprehensively in this work.

3.1. Effect of Slag Basicity

In this section, the effect of quaternary slag basicity on metal grade and recovery of ferronickel was investigated in 1.0 of stoichiometric carbon of reductant addition. The smelting process was carried out at temperature of 1450-1500°C for 60 minutes. Figure 3 shows that the nickel grade increased from 0.6 to 0.8 of slag basicity and then decreased to 1.2. The optimum nickel grade, i.e., 10.27 %, is obtained from 0.8 of basicity due to the decrease of iron recovery with a relatively similar yield compared with 0.6 basicity. In ferronickel production, the nickel grade is inversely proportional to iron recovery. However, the lowest iron recovery, obtained at 1.2 of basicity, does not affect the improvement of nickel grade. The lowest yield at this basicity indicates that the metal oxide reduction did not work well. This could be due to the passivation in the form of layers containing high melting point phases that hampered the diffusion of the reductant to the metal oxide matrix.

The carbon content increases with the increase of slag basicity. It indicates that the activity of carbon increases with the increasing of basicity, which promotes the diffusion of carbon into ferronickel. Although the presence of carbon could lower the melting point of ferroalloys, too much carbon could suppress the nickel grade in ferronickel. It also contributes more effort to the decarburization process of stainless steel production. The Silicon content in ferronickel decreases with the increase of slag basicity. Silicon is an "acid" element and therefore has low activitywhen the slag is highly basic. At 0.8 slag basicity, the silicon grade is relatively high. This information is very important for selecting refractory materials containing high-SiO_2 or acid refractory. Carbon brick is commonly used for refractory in the hearth area of arc furnaces in the ferronickel smelting process due to its good performance in a wide range of basicity (acid and basic).

According to the XRD analysis of basicity at 0.6 (Figure 4), the slag mostly consists of forsterite, pyroxene, and diopside. Basic oxide, such as calcium oxide, could break the magnesium silicate structure, which is transformed into diopside, releasing the iron and nickel to form fayalite, as expressed in reaction (16). Fayalite is not found in Figure 4, which indicates that the 1.0 stoichiometric of reductant is sufficient to reduce all fayalite into ferronickel, as expressed in reaction (17) [23]. Pyroxene is not found at basicity 0.8, which might be transformed into diopside. The melting point of the diopside is 1391 °C [24-25]. It is lower than forsterite and pyroxene, about 1420-1680 °C [26]. Therefore, diopside contributes to lowering the energy consumption in the smelting process. Heating the slag above its melting temperature will decrease the viscosity, positively affecting metal-slag segregation and resulting in high yield and metal recovery [27-28]. Thus, a smelting temperature of about 1450-1500 °C in nickel processing is mostly applied to the slag-containing diopside. At higher basicity, melilite, and monticellite are found. The intensity of these two
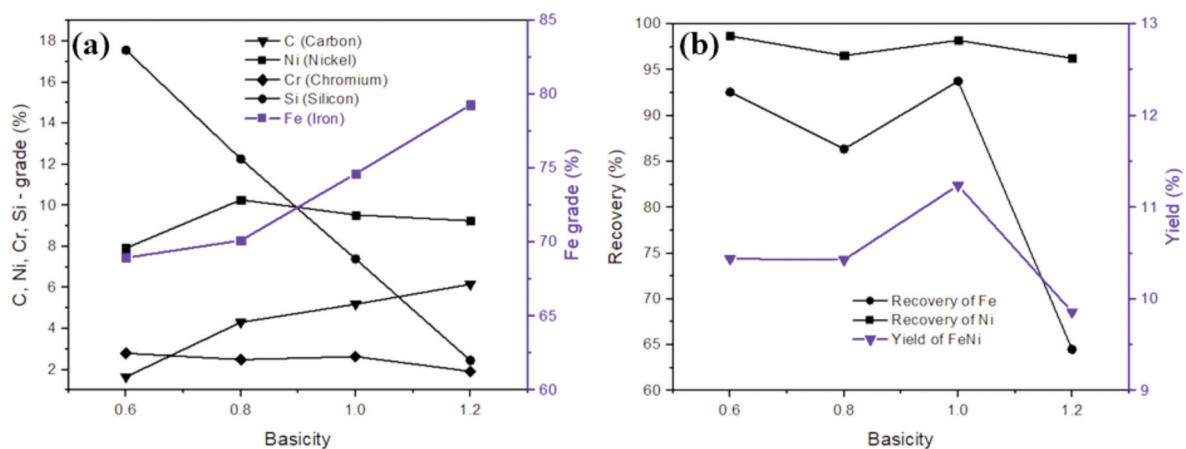

Figure 3. *Effect of slag basicity on (a) metal grade; (b) recovery and yield of ferronickel*

phases increases with the increase of basicity. The transformation of diopside to melilite and monticellite is described in reactions (18-19). Melilite and monticellite have a higher melting point than diopside. The presence of these phases in large intensity will increase the slag viscosity, negatively affecting the nickel grade and recovery, as can be found at 1.2 basicity in Figure 3. Therefore, the optimum basicity in this smelting of nickel laterite using a DC-arc furnace is obtained at 0.8 with mostly diopside in slag.
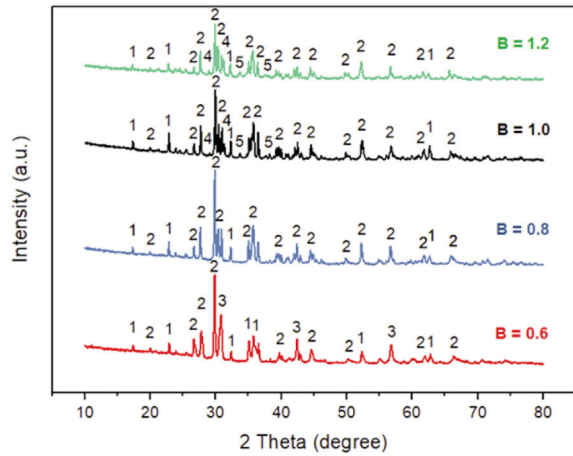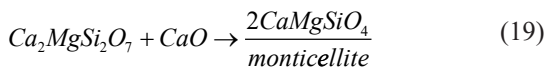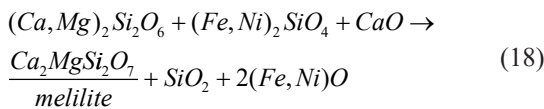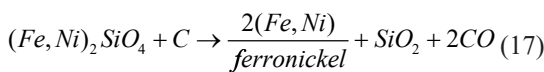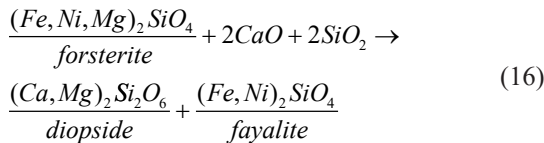

Figure 4. The XRD analysis of slag with various basicity. 1-forsterite (Fe,Ni,Mg)$_2$SiO$_4$, 2-diopside ((Ca,Mg)$_2$Si$_2$O$_6$), 3-pyroxene-((Fe,Mg,Ni)SiO$_3$), 4-melilite (Ca$_2$MgSi$_2$O$_7$), 5-monticellite (CaMgSiO$_4$)

$$\underset{forsterite}{(Fe,Ni,Mg)_2SiO_4} + 2CaO + 2SiO_2 \rightarrow$$

$$\underset{diopside}{(Ca,Mg)_2Si_2O_6} + \underset{fayalite}{(Fe,Ni)_2SiO_4} \quad (16)$$

$$(Fe,Ni)_2SiO_4 + C \rightarrow \underset{ferronickel}{2(Fe,Ni)} + SiO_2 + 2CO \quad (17)$$

$$(Ca,Mg)_2Si_2O_6 + (Fe,Ni)_2SiO_4 + CaO \rightarrow$$
$$\underset{melilite}{Ca_2MgSi_2O_7} + SiO_2 + 2(Fe,Ni)O \quad (18)$$

$$Ca_2MgSi_2O_7 + CaO \rightarrow \underset{monticellite}{2CaMgSiO_4} \quad (19)$$

According to Luo et al. [24], the Al$_2$O$_3$ content in the slag from the smelting process of saprolitic nickel ore is generally below 10 %, due to the less 5% of Al$_2$O$_3$ content in saprolite. This is consistant with the composition of the slag from this smelting process, as listed in Table 6. Therefore, it is appropriate to plot the chemical composition of slag into the pseudo-ternary diagram of CaO-MgO-SiO$_2$-5%Al$_2$O$_3$, as shown in Figure 5, is carried out to observe the effect of CaO addition on the phase of slag formation in this smelting process. From Figure 5, the addition of CaO initially promotes the formation of low melting point

diopside. Furthermore, the increasing of CaO, which also increasing the basicity, will generate the high melting point phase, such as monticellite. It is agreed with the XRD analysis in Figure 4. Lowering the melting point of the slag will be affected to the low temperature of smelting process. This reduces energy consumption, which could increase economic feasibility, and reduces gas emissions from the smelting process of low-grade saprolitic nickel ore.

Table 6. Chemical composition of slag with various basicity

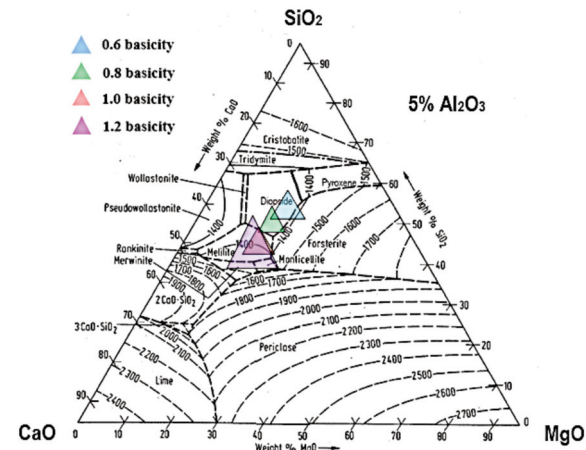| Basicity of slag	Chemical Composition (wt %)			
	CaO	MgO	SiO$_2$	Al$_2$O$_3$
0.6	21.968	16.908	52.927	3.967
0.8	27.19	16.657	46.789	3.168
1	34.837	14.602	42.178	5.47
1.2	33.942	10.765	35.965	2.539

Figure 5. Pseudo-ternary diagram of CaO-MgO-SiO$_2$ - 5%Al$_2$O$_3$ [29]

From microstructure analysis (Figure 6), lamellar black graphite is observed, which is due to the high carbon and silicon content in ferronickel, which acts as a graphite-forming element in ferrous materials [30]. The presence of graphite also makes the ferronickel brittle. The volume of graphite appeared to decrease with the increase of basicity due to the decreasing silicon content, a graphite-forming element in ferrous materials [31]. Lamellae graphite becomes coarser with increased basicity due to the increased carbon content. However, the higher the carbon contents in ferrous materials, the lower its melting point.Therefore, it has a positive effect on the smelting process of nickel ore.

3.2. Effect of reductant dosage

To investigate the effect of reductant dosage, various 0.6 to 1.2 soichiometric reductants were
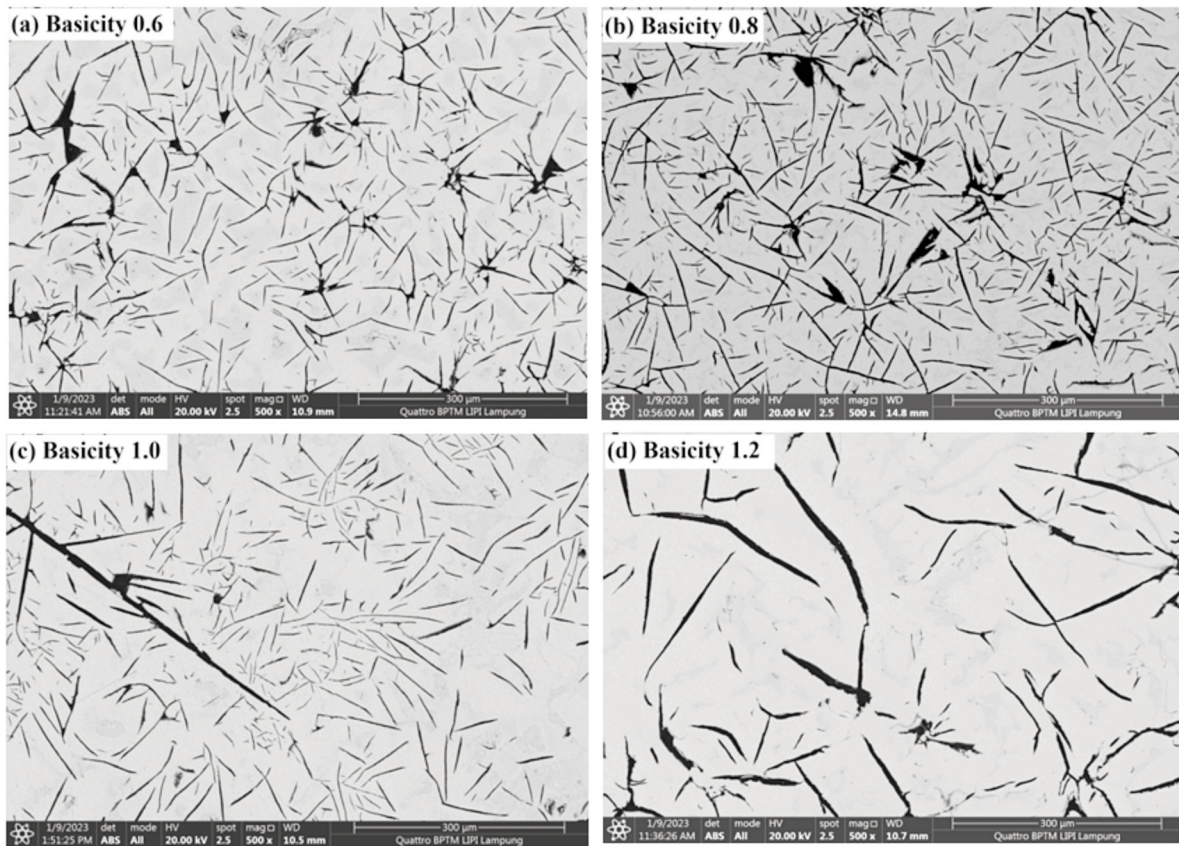
Figure 6. Microstructure analysis of ferronickel with various basicity

used in this smelting process at temperature of 1450-1500°C for 60 minutes with the basicity of slag being 0.8. Figure 7 shows the effect of reductant dosage on the metal grade of ferronickel. At 0.6 stoichiometry, almost all metallic elements (Fe, Ni, Cr, and Si) have low grades due to low carbon to reduce the metal oxide. Furthermore, the nickel grade increases from 0.6 to 0.8 stoichiometry of reductant. However, it decreases significantly at 1.0

stoichiometry due to the sharp increases of silicon grade suppressing the nickel grade. From the Ellingham diagram, as shown in Figure 8, the silicon dioxide line is lower than nickel oxide, making it more challenging to reduce. The reduction of silicon dioxide to silicon is shown in reactions (20-22) [32]. The minimum temperature reductant of silicon dioxide is demonstrated by the cross line with carbon monoxide, which is about 1600 °C. In an arc
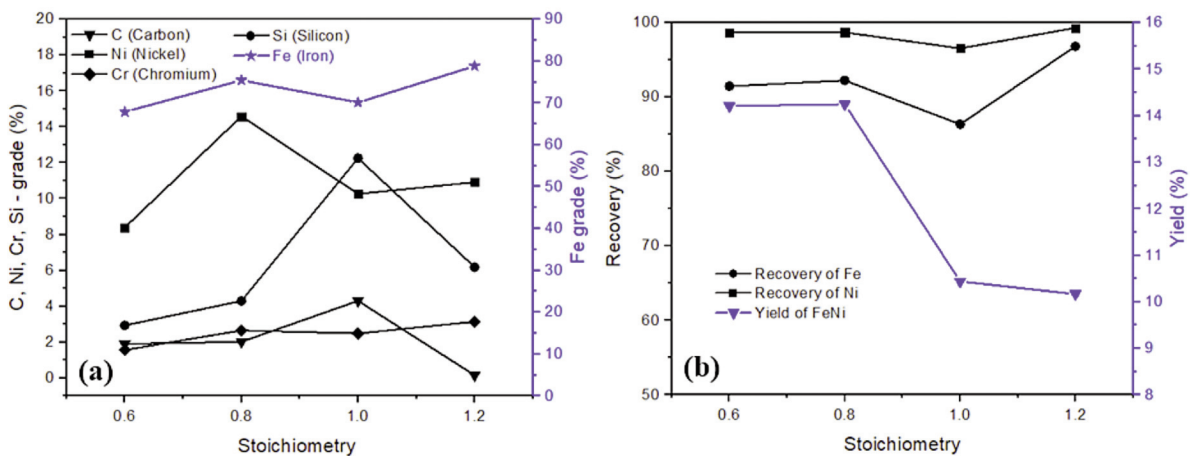

Figure 7. Effect of reductant dosage on (a) metal grade; (b) recovery and yield of ferronickel

furnace, the temperature in the arc zone is very high, which could reach more than 2000 °C. Therefore, although the liquidus temperature in the DC-arc furnace is 1400-1500 °C, silicon dioxide reduction could occur in the arc zone with a sufficient reductant amount. However, the silicon grade decreases significantly from 1.0 to 1.2 due to the significantly increased iron and chromium grade. It indicates the reductant is mostly used for reducing iron oxide to metallic iron at 1.2 stoichiometry. The carbon content in ferronickel also has a similar trend with silicon. According to Jones et al., a proper amount of reductant should be added to obtain high-grade ferronickel. The morereducing agents are added , the more other metal or metalloid (such as iron, chromium, and silicon) oxide will be transformed into a metallic phase, which could suppress the nickel grade in ferronickel [16].

$$SiO_2 + C \rightarrow SiO + CO \qquad (20)$$

$$SiO + 2C \rightarrow SiC + CO \qquad (21)$$

$$SiO + SiC \rightarrow 2Si + CO \qquad (22)$$

$$SiC + 2Fe \rightarrow Fe_2Si + C \qquad (23)$$

Figure 7(b) shows that the nickel recovery reached above 95% in this smelting of nickel laterite. The highest recovery of nickel was obtained at 0.8 stoichiometry, namely 92.26%. The recovery of iron increases with the increase of reductant dosage. Nickel oxide has a lower-temperature reduction than iron oxide, as illustrated in Figure 8. Thus, limited reductant addition could suppress the iron recovery, increasing the concentrate's nickel grade. The yield recovery decreases significantly after 0.8 stoichiometry. The cokes contain high ash, as listed in Table 3. Mostly, ash from coals or coke combustion
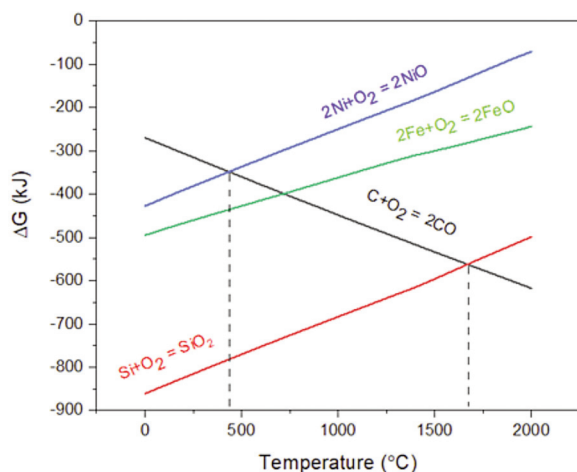

Figure 8. *Ellingham diagram of NiO, CO, and SiO₂*

consists of aluminum and silicon dioxide. Thus, increasing reductant addition will increase the ash volume, which could generate improper slag basicity resulting in low yield production of ferronickel.

From XRD analysis, as described in Figure 9, the slag mostly consisted of diopside. The presence of diopside promotes smelting temperature due to its low melting point temperature, i.e., 1391 °C. It is affected by the low viscosity of slag, which promotes the optimum segregation of ferronickel from slag. Therefore, a high recovery of nickel (more than 90%) is obtained from this smelting process (at the basicity of 0.8 with different reductant dosages). However, a small intensity of forsterite is found. It has a higher melting point temperature (i.e., 1890 °C) than diopside. The presence of forsterite will suppress the nickel grade and recovery. The intensity of forsterite decreases from 0.6 to 0.8 stoichiometry of reductant resulting in optimum nickel grade and yield of ferronickel. Nevertheless, it decreases from 0.8 to 1.2 stoichiometry of reductant. The increasing intensity of forsterite might be caused by the increasing amount of silicon dioxide coming from impurities or ashes of coke; thus, excess silicon dioxide will be reacted with magnesium oxide from nickel laterite to form forsterite.
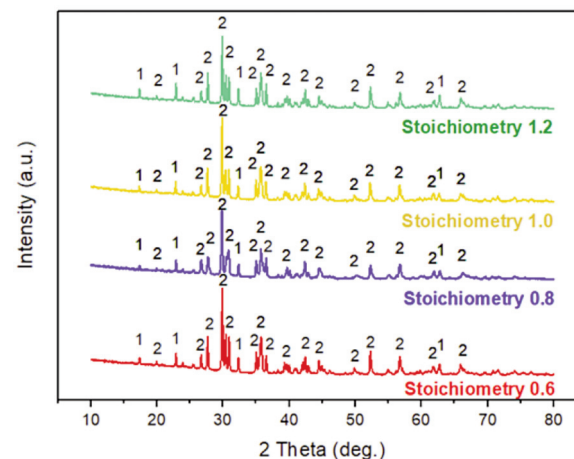

Figure 9. *XRD analysis of ferronickel slag with various dosages of reductant*

The microstructure analysis of ferronickel from the smelting of nickel laterite with various reductant dosages is shown in Figure 10. Graphite appeared in black-needle and irregular shape. The intensity of graphite increases with the increase of stoichiometry from 0.6 to 1.0. It is due to the increase of silicon, which improves the activity of carbon to form graphite, as expressed in reaction (23). Nevertheless, the volume of graphite is decreased at stoichiometry 1.2, where most of the silicon is transformed into forsterite.
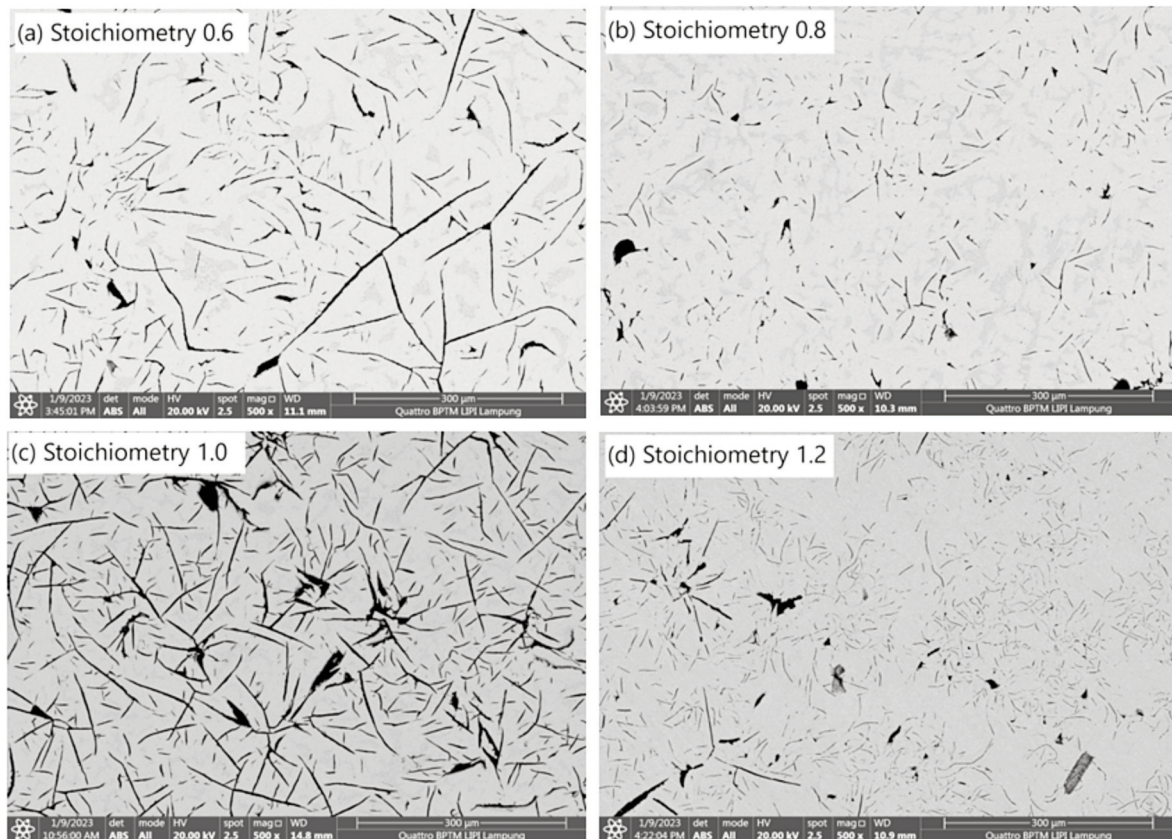
Figure 10. Microstructure of ferronickel with various stoichiometry of reductant

4. Conclusion

The optimum of quaternary slag basicity for smelting nickel ore in a DC-arc furnace is 0.8 due to the formation of a low melting point phase, i.e., diopside. Increasing basicity generated higher melting point phases, such as melilite/merwinite and monticellite, which could negatively affect nickel grade and recovery. It could also result in high energy consumption in this smelting process. The silicon content in ferronickel decreased with the increasing slag basicity, while the carbon content increased. It led to a coarser graphite formation in the microstructure, contributing to the metallic iron's low melting temperature. The reductant must be added to reduce the nickel oxide in saprolitic nickel ore completely but limited reduced for iron oxide. The higher nickel content in ferronickel was found at 0.8 of stoichiometric carbon of coke addition. This optimum condition (0.8 basicity with 0.8 stoichiometry) has produced ferronickel containing 14.59% Ni grade with 92.26% recovery.

Author's Contributions

F. Nurjaman, F. Bahfie, and B. Suharno provided the financial support, designed the experiment and conducted data analysis. B. Septiansyah, A. S. Handoko, H. Z. Hakim, L. O. Arham, and Y. Sari conducted the experiment and wrote the manuscript. I. Suherman, H. Haryadi, and T. Suseno provided constructive suggestions for the manuscript.

Data Availability

The data used to support the findings of this study are available from the corresponding author upon request.

Conflict of Interest

On behalf of all authors, the corresponding author states that there is no conflict of interest.

References

[1] W. Lv, Y. Xin, R. Elliot, J. Song, X. Lv., M. Barati, Drying kinetics of a Philippine nickel laterite ore by microwave heating, Mineral Processing and Extractive Metallurgy Review, 42 (2020) 46-52. https://doi.org/10.1080/08827508.2020.1801433

[2] G. Li, H. Jia, J. Luo, Z. Peng, Y. Zhang, T. Jiang, Ferronickel preparation from nickeliferous laterite by rotary kiln-electric furnace process, in Characterization of Minerals, Metals, and Materials, Springer Cham., 2016, p. 143-150. https://doi.org/10.1007/978-3-319-48210-1_17

[3] B. K. Tsang, Y. Zhang, Energy challenges for a nickel laterite mining and smelting facility, Proc. 3rd IFAC Workshop on Automation in the Mining, Mineral and Metal Industries, 10-12 Sepetember 2012, Gifu, Japan, 2012, p.7-12.

[4] G. M. Mudd, Global trends and environmental issues in nickel mining: Sulfides versus laterites, Ore Geology Reviews, 38 (2010) 9-26. https://doi.org/10.1016/j.oregeorev.2010.05.003

[5] M. G. King, Nickel laterite technology-Finally a new dawn, JOM, 57 (2005) 35-39. https://doi.org/10.1007/s11837-005-0250-7

[6] E. N. Zevgolis, K. A. Daskalakis, The nickel production methods from laterites and the Greek ferronickel production among them, Material Proceedings, 5 (2021) 1-12. https://doi.org/10.3390/materproc2021005104

[7] D. A. Quintero-Coronel, W. D. Guillin-Estrada, J. L. Echeverri-Roman, H. Maury, L. Corredor, J. A. Ruiz, B. S. Rueda, A. Gonzalez-Quiroga, Large- and particle-scale energy assessment of reduction roasting of nickel laterite ore for ferronickel production via the rotary kiln-electric furnace process, Thermal Science and Engineering Progress, 32 (101331) (2022) 1-14. https://doi.org/10.1016/j.tsep.2022.101331

[8] L. J. Erasmus, and L. J. Fourie, ESS smelting technology enabling FeNi smelting from limonite, Proc. The Fourteenth International Ferroalloys Congress: Energy efficiency and environmental friendliness are the future of the global ferroalloys industry, 31 May-4 June 2015, Kiev, Ukraine, 2015, p. 210-218.

[9] I. J. Koetze, Pilot plant production of ferronickel from nickel oxide ores and dusts in a DC arc furnace, Minerals Engineering, 15 (2002) 1017-1022. https://doi.org/10.1016/S0892-6875(02)00127-9

[10] A. Oxley, N. Barcza, Hydro-pyro integration in the processing of nickel laterites, Minerals Engineering, 54 (2013) 2-13. https://doi.org/10.1016/j.mineng.2013.02.012

[11] J. Luo, G. Li, M. Rao, Z. Peng, G. Liang, T. Jiang, X. Guo, Control of slag formation in the electric furnace smelting of ferronickel for an energy-saving production, Journal of Cleaner Production, 287 (125082) (2021) 1-12. https://doi.org/10.1016/j.jclepro.2020.125082

[12] R. Andika, W. Astuti, Syafriadi, and F. Nurjaman, Effect of flux adiition and reductant type in smelting process of Indonesian limonite ore in electric arc furnace, IOP Conf. Series: Materials Science Engineering 478 (012007) (2019) 1-7. https://doi.org/10.1088/1757-899X/478/1/012007

[13] W. Wei, P. B. Samuelsson, P. G. Jonsson, R. Gyllenram, and B. Glaser, Energy consumption and greenhouse gas emissions of high-carbon ferrochrome production, JOM, 75 (2023) 1206-1220. https://doi.org/10.1007/s11837-023-05707-8

[14] J. Z. khoo, N. Haque, S. Bhattacharya, Process simulation and exergy analysis of two nickel laterite processing technologies, International Journal of Mineral Processing, 161 (2017) 83-93. https://doi.org/10.1016/j.minpro.2017.02.012

[15] P. Liu, B. Li, S. C. P. Cheung, W. Wu, Material and energy flows in rotary kiln-electric furnace smelting of ferronickel alloy with energy saving, Applied Thermal Engineering, 109 (2016) 542-559. https://doi.org/10.1016/j.applthermaleng.2016.08.095

[16] R. T. Jones, Reductive smelting for the recovery of nickel in a DC arc furnace, Proc. of 7th European Metallurgical Conference 2013, 23-26 June 2013, Weimar, Germany, p. 1019-1026.

[17] E. Keskinkilic, Nickel laterite smelting process and some examples of recent possible modifications to the conventional route, Metals, 9 (974) (2019) 1-16. https://doi.org/10.3390/met9090974

[18] R. T. Jones, Q. G. Reynolds, T. R. Curr, and D. Sager, Some myths about DC arc furnaces, The Journal of The Southern African Institute of Mining and Metallurgy, 111 (2011), 665-674. https://www.saimm.co.za/Journal/v111n10p665.pdf

[19] R. T. Jones, DC arc furnaces-Past, present, and future, in celebrating the megascale, Springer Cham, 2014, p. 129-139. https://doi.org/10.1007/978-3-319-48234-7_10

[20] F. Nurjaman, F., W Astuti, F. Bahfie, & B. Suharno, Study of selective reduction in lateritic nickel ore: Saprolite versus limonite, Materials Today: Proceedings 44 (2021) 1488-1494. https://doi.org/10.1016/j.matpr.2020.11.687.

[21] C. A. Pickles, W. Anthony, Thermodynamic modelling of the reduction of a saprolitic laterite ore by methane, Minerals Engineering, 120 (2018) 47-59. https://doi.org/10.1016/j.mineng.2018.02.006.

[22] Z. Wang, M. Chu, Z. Liu, H. Wang, W. Zhao, and L. Gao, Preparing ferro-nickel alloy from low-grade laterite nickel ore based on metallized reduction–magnetic separation, Metals, 7 (2017) 1-14. https://doi.org/10.3390/met7080313.

[23] H. Wang, L. Shen, H. Bao, W. Zhang, X. Zhang, L. Luo and S. Song, Investigation of solid-state carbothermal reduction of fayalite with and without added metallic iron, JOM, 73 (2021) 703-711. https://doi.org/10.1007/s11837-020-04515-8.

[24] J. Luo, G. Li, M. Rao, Z. Peng, G. Liang, T. Jiang, X. Guo, Control of slag formation in the electric furnace smelting of ferronickel for an energy-saving production, Journal of Cleaner Production, 287 (2021) 1-12. https://doi.org/10.1016/j.jclepro.2020.125082.

[25] H. S. Yoder, Change of melting point of diopside with pressure, The Journal of Geology, 60 (1952) 364-374. https://doi.org/10.1086/625984

[26] F. Nurjaman, Y. Sari, P. Manurung, A. S. Handoko, F. Bahfie, W. Astuti, B. Suharno, Study of binary, ternary, and quaternary basicity in reduction of saprolitic nickel ore, Transactions of the Indian Institue of Metals, 74 (2021) 3249-3263. https://doi.org/10.1007/s12666-021-02391-7

[27] X. M. Lv, J. Qiu, M. Liu. M. Liu., X. W. Lv, Viscosity of SiO2-MgO-Al2O3-FeO slag for nickel laterite

smelting process. Proc. The Fourteenth International Ferroalloys Congress: Energy efficiency and environmental friendliness are the future of the global ferroalloys industry, 31 May-4 June 2015, Kiev, Ukraine, 2015, p. 561-566.

[28] X. M. Lv, X. W. Lv., L. W. Wang, J. Qiu, M. Liu, Viscosity and structure evolution of the SiO_2-MgO-FeO-CaO-Al_2O_3 slag in ferronickel smelting process from laterite, Journal of Mining and Metallurgy Section B: Metallurgy, 53 (2) B (2017) 147-154. https://doi.org/10.2298/JMMB150911002L.

[29] M. Allibert, H. Gaye, J. Geiseler, D. Janke, B. J. Keene, D. Kirner, M. Kowalski, J. Lehmann, K. C. Mills, D. Neuschutz, R. Parra, C. Saint-Jours, P. J. Spencer, M. Susa, M. Tmar, E. Woermann, Slag Atlas 2nd Edition, Stahlinstitut VDEh, Germany 1995, p. 156.

[30] J. H. Park, Structure-property relationship of CaO-MgO-SiO2 slag: Quantitaive analysis of Raman spectra, Metallurgical and Materials Transactions B,

44B (2013) 938-947. https://doi.org/10.1007/s11663-013-9825-9

[31] B. S. Terry, O. S. Chinyamakobvu, Assessment of the reaction of SiC powders with iron based alloys, Journal of Materials Science, 28 (1993) 6779-6784. https://doi.org/10.1007/BF00356431

[32] B. Abolpour, and R. Shamsoddini, Mechanism of reaction of silica and carbon for producing silicon carbide, Progress in Kinetics and Mechanism, 45 (2019) 1-14. https://doi.org/10.1177/1468678319891416.

TOPLJENJE SIROMAŠNE RUDE SAPROLITNOG NIKLA U DC-ELEKTROLUČNOJ PEĆI

F. Nurjaman [a, *], H.Z. Hakim [b], B. Septiansyah [b], L.O. Arham [b], A.S. Handoko [a], F. Bahfie [a], I. Suherman [a], H. Haryadi [a], T. Suseno [a], Y. Sari [a], B. Suharno [c]

[a] Nacionalna agencija za istraživanje i inovacije, Istraživački centar za rudarsku tehnologiju, Južni Lampung, Indonezija
[b] Tehnološki institut Sumatera, Odeljenje za rudarsko inženjerstvo, Južni Lampung, Indonezija
[c] Universitas Indonesia, Odsek za metalurgiju i materijale, Depok, Indonezija

Apstrakt

Većina topljenja laterita nikla za proizvodnju feronikla se vrši pomoću elektrolučne peći na naizmeničnu struju. Iako je DC elektrolučna peć pogodna za topljenje fine rude, retko se koristi za nikl laterit. U ovom radu su detaljno proučavani efekti bazičnosti šljake i stehiometrije dodavanja reducenata pri topljenju siromašne rude saprolitnog nikla na sadržaj i dobijanje nikla, prinos kao i na i faze šljake. Proces topljenja je sproveden u laboratorijskoj elektrolučnoj peći na jednosmernu struju sa jednom elektrodom prečnika 30 cm. 5 kg saprolitne rude nikla niskog kvaliteta (1,92 Ni-12,97 Fe), nešto koksa kao reducenata i nešto krečnjaka kao topitelja topljeno je u DC elektrolučnoj peći oko jedan sat. Temperatura izlivanja tečnog metala i šljake bila je 1400-1500°C. Bazičnost kvaternarne šljake od 0,8 i stehiometrijskog ugljenika reducenata od 0,8 rezultirali su optimalnim procesom topljenja rude nikla u DC elektrolučnoj peći, pri čemu se dobija feronikl sa sadržajem Ni od 14,59% sa iskorišćenjem 92,26%.

Ključne reči: Laterit nikla; Topljenje; DC elektrolučna peć; Feronikl